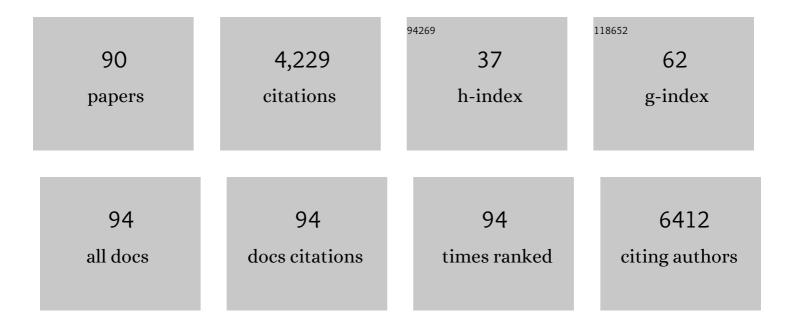
Xianjue Chen

List of Publications by Year in descending order

Source: https://exaly.com/author-pdf/4673276/publications.pdf Version: 2024-02-01



XIANILIE CHEN

#	Article	IF	CITATIONS
1	Interaction of Black Phosphorus with Oxygen and Water. Chemistry of Materials, 2016, 28, 8330-8339.	3.2	436
2	Vortex fluidic exfoliation of graphite and boron nitride. Chemical Communications, 2012, 48, 3703.	2.2	245
3	Capturing the active sites of multimetallic (oxy)hydroxides for the oxygen evolution reaction. Energy and Environmental Science, 2020, 13, 4225-4237.	15.6	186
4	Large-area single-crystal AB-bilayer and ABA-trilayer graphene grown on a Cu/Ni(111) foil. Nature Nanotechnology, 2020, 15, 289-295.	15.6	141
5	Ultrafast Aqueous Potassiumâ€ion Batteries Cathode for Stable Intermittent Gridâ€Scale Energy Storage. Advanced Energy Materials, 2018, 8, 1801413.	10.2	136
6	<i>Operando</i> Raman Spectroscopy Reveals Cr-Induced-Phase Reconstruction of NiFe and CoFe Oxyhydroxides for Enhanced Electrocatalytic Water Oxidation. Chemistry of Materials, 2020, 32, 4303-4311.	3.2	115
7	Nitrate removal from liquid effluents using microalgae immobilized on chitosan nanofiber mats. Green Chemistry, 2012, 14, 2682.	4.6	114
8	Surface Reconstruction of Ultrathin Palladium Nanosheets during Electrocatalytic CO ₂ Reduction. Angewandte Chemie - International Edition, 2020, 59, 21493-21498.	7.2	97
9	Optimising a vortex fluidic device for controlling chemical reactivity and selectivity. Scientific Reports, 2013, 3, 2282.	1.6	93
10	Controlled Folding of Single Crystal Graphene. Nano Letters, 2017, 17, 1467-1473.	4.5	92
11	Nitrogen Vacancy Induced Coordinative Reconstruction of Singleâ€Atom Ni Catalyst for Efficient Electrochemical CO ₂ Reduction. Advanced Functional Materials, 2021, 31, 2107072.	7.8	89
12	Graphitization of graphene oxide films under pressure. Carbon, 2018, 132, 294-303.	5.4	84
13	Efficient Oxygen Evolution and Gas Bubble Release Achieved by a Low Gas Bubble Adhesive Iron–Nickel Vanadate Electrocatalyst. Small, 2020, 16, e2002412.	5.2	77
14	Shear induced formation of carbon and boron nitride nano-scrolls. Nanoscale, 2013, 5, 498-502.	2.8	68
15	Rapid thermal decomposition of confined graphene oxide films in air. Carbon, 2016, 101, 71-76.	5.4	65
16	Role of Graphene in Water-Assisted Oxidation of Copper in Relation to Dry Transfer of Graphene. Chemistry of Materials, 2017, 29, 4546-4556.	3.2	63
17	Biogenic production of palladium nanocrystals using microalgae and their immobilization on chitosan nanofibers for catalytic applications. RSC Advances, 2013, 3, 1009-1012.	1.7	60
18	Functional multi-layer graphene–algae hybrid material formed using vortex fluidics. Green Chemistry, 2013, 15, 650.	4.6	60

#	Article	IF	CITATIONS
19	High valence chromium regulated cobalt-iron-hydroxide for enhanced water oxidation. Journal of Power Sources, 2018, 402, 381-387.	4.0	60
20	p-Phosphonic acid calix[8]arene assisted exfoliation and stabilization of 2D materials in water. Chemical Communications, 2012, 48, 11407.	2.2	58
21	Ultrahigh Areal Capacity Hydrogenâ€ion Batteries with MoO ₃ Loading Over 90 mg cm ^{â^²2} . Advanced Functional Materials, 2020, 30, 2005477.	7.8	57
22	Controlling the Thickness of Thermally Expanded Films of Graphene Oxide. ACS Nano, 2017, 11, 665-674.	7.3	55
23	Pyrene-conjugated hyaluronan facilitated exfoliation and stabilisation of low dimensional nanomaterials in water. Chemical Communications, 2013, 49, 4845.	2.2	54
24	Confinement of Ionic Liquids at Single-Ni-Sites Boost Electroreduction of CO ₂ in Aqueous Electrolytes. ACS Catalysis, 2020, 10, 13171-13178.	5.5	54
25	Co-Fe binary metal oxide electrocatalyst with synergistic interface structures for efficient overall water splitting. Catalysis Today, 2020, 351, 44-49.	2.2	52
26	Metal–Sulfur Linkages Achieved by Organic Tethering of Ruthenium Nanocrystals for Enhanced Electrochemical Nitrogen Reduction. Angewandte Chemie - International Edition, 2020, 59, 21465-21469.	7.2	52
27	A zero-dimensional nickel, iron–metal–organic framework (MOF) for synergistic N ₂ electrofixation. Journal of Materials Chemistry A, 2020, 8, 18810-18815.	5.2	52
28	Porous Two-Dimensional Monolayer Metal–Organic Framework Material and Its Use for the Size-Selective Separation of Nanoparticles. ACS Applied Materials & Interfaces, 2017, 9, 28107-28116.	4.0	51
29	Entrapment of Chlorella vulgaris cells within graphene oxide layers. RSC Advances, 2013, 3, 8180.	1.7	50
30	Controlling nanomaterial synthesis, chemical reactions and self assembly in dynamic thin films. Chemical Society Reviews, 2014, 43, 1387-1399.	18.7	50
31	Synergistic bimetallic CoFe ₂ O ₄ clusters supported on graphene for ambient electrocatalytic reduction of nitrogen to ammonia. Chemical Communications, 2019, 55, 12184-12187.	2.2	50
32	Ultrastiff, Strong, and Highly Thermally Conductive Crystalline Graphitic Films with Mixed Stacking Order. Advanced Materials, 2019, 31, e1903039.	11.1	49
33	Ni2P@carbon core-shell nanorod array derived from ZIF-67-Ni: Effect of phosphorization temperature on morphology, structure and hydrogen evolution reaction performance. Applied Surface Science, 2018, 457, 933-941.	3.1	48
34	(N, B) Dual Heteroatom-Doped Hierarchical Porous Carbon Framework for Efficient Electroreduction of Carbon Dioxide. ACS Sustainable Chemistry and Engineering, 2020, 8, 6003-6010.	3.2	45
35	Non-covalently modified graphene supported ultrafine nanoparticles of palladium for hydrogen gas sensing. RSC Advances, 2013, 3, 3213.	1.7	44
36	A versatile approach for decorating 2D nanomaterials with Pd or Pt nanoparticles. Chemical Communications, 2013, 49, 1160-1162.	2.2	43

#	Article	IF	CITATIONS
37	Raman Spectral Band Oscillations in Large Graphene Bubbles. Physical Review Letters, 2018, 120, 186104.	2.9	43
38	Defective Indium/Indium Oxide Heterostructures for Highly Selective Carbon Dioxide Electrocatalysis. Inorganic Chemistry, 2020, 59, 12437-12444.	1.9	40
39	Synthesis of nanocrystalline Mg-based Mg–Ti composite powders by mechanical milling. Materials Characterization, 2015, 106, 44-51.	1.9	38
40	Vertical Growth of Porous Perovskite Nanoarrays on Nickel Foam for Efficient Oxygen Evolution Reaction. ACS Sustainable Chemistry and Engineering, 2020, 8, 4863-4870.	3.2	38
41	Self-Supported NiSe ₂ Nanowire Arrays on Carbon Fiber Paper as Efficient and Stable Electrode for Hydrogen Evolution Reaction. ACS Sustainable Chemistry and Engineering, 2018, 6, 11884-11891.	3.2	37
42	Nanostructured amalgams with tuneable silver–mercury bonding sites for selective electroreduction of carbon dioxide into formate and carbon monoxide. Journal of Materials Chemistry A, 2019, 7, 15907-15912.	5.2	37
43	Surface Reconstruction of Ultrathin Palladium Nanosheets during Electrocatalytic CO ₂ Reduction. Angewandte Chemie, 2020, 132, 21677-21682.	1.6	37
44	Metal-cation-modified graphene oxide membranes for water permeation. Carbon, 2020, 170, 646-657.	5.4	35
45	Amphiphilic graphene oxide stabilisation of hexagonal BN and MoS ₂ sheets. Chemical Communications, 2015, 51, 11709-11712.	2.2	34
46	Sub-micron moulding topological mass transport regimes in angled vortex fluidic flow. Nanoscale Advances, 2021, 3, 3064-3075.	2.2	34
47	High performance graphene embedded rubber composites. RSC Advances, 2015, 5, 81707-81712.	1.7	33
48	Tuning the surface energy density of non-stoichiometric LaCoO3 perovskite for enhanced water oxidation. Journal of Power Sources, 2020, 478, 228748.	4.0	33
49	Shear flow assisted decoration of carbon nano-onions with platinum nanoparticles. Chemical Communications, 2013, 49, 5171.	2.2	32
50	Shear induced fabrication of intertwined single walled carbon nanotube rings. Chemical Communications, 2014, 50, 11295-11298.	2.2	32
51	Hierarchical Patterning of Multifunctional Conducting Polymer Nanoparticles as a Bionic Platform for Topographic Contact Guidance. ACS Nano, 2015, 9, 1767-1774.	7.3	32
52	Shear induced carboplatin binding within the cavity of a phospholipid mimic for increased anticancer efficacy. Scientific Reports, 2015, 5, 10414.	1.6	30
53	Multifunctional Macroassembled Graphene Nanofilms with High Crystallinity. Advanced Materials, 2021, 33, e2104195.	11.1	30
54	Nitrate uptake by p-phosphonic acid calix[8]arene stabilized graphene. Chemical Communications, 2013, 49, 8172.	2.2	26

#	Article	IF	CITATIONS
55	Microwave-Induced Plasma Synthesis of Defect-Rich, Highly Ordered Porous Phosphorus-Doped Cobalt Oxides for Overall Water Electrolysis. Journal of Physical Chemistry C, 2020, 124, 9971-9978.	1.5	26
56	Liquid-phase exfoliation of F-diamane-like nanosheets. Carbon, 2021, 175, 124-130.	5.4	26
57	Wrinkle networks in exfoliated multilayer graphene and other layered materials. Carbon, 2020, 156, 24-30.	5.4	23
58	Unravelling the structure and function of human hair. Green Chemistry, 2013, 15, 1268.	4.6	22
59	Vitamin B ₁₂ on Graphene for Highly Efficient CO ₂ Electroreduction. ACS Applied Materials & Interfaces, 2020, 12, 41288-41293.	4.0	22
60	Aqueous based synthesis of antimicrobial-decorated graphene. Journal of Colloid and Interface Science, 2015, 443, 88-96.	5.0	20
61	Shock Exfoliation of Graphene Fluoride in Microwave. Small, 2020, 16, e1903397.	5.2	20
62	Template-free assembly of three-dimensional networks of graphene hollow spheres at the water/toluene interface. Journal of Colloid and Interface Science, 2014, 430, 174-177.	5.0	19
63	Microencapsulation of bacterial strains in graphene oxide nano-sheets using vortex fluidics. RSC Advances, 2015, 5, 37424-37430.	1.7	19
64	p-Phosphonic acid calix[8]arene assisted dispersion and stabilisation of pea-pod C ₆₀ @multi-walled carbon nanotubes in water. Chemical Communications, 2015, 51, 2399-2402.	2.2	19
65	Functional noble metal nanostructures involving pyrene-conjugated-hyaluronan stabilised reduced graphene oxide. RSC Advances, 2013, 3, 25166.	1.7	17
66	Dual-responsive, Methotrexate-loaded, Ascorbic acid-derived Micelles Exert Anti-tumor and Anti-metastatic Effects by Inhibiting NF-κB Signaling in an Orthotopic Mouse Model of Human Choriocarcinoma. Theranostics, 2019, 9, 4354-4374.	4.6	17
67	Self-assembled calixarene aligned patterning of noble metal nanoparticles on graphene. Nanoscale, 2014, 6, 4517-4520.	2.8	16
68	Liquid-phase water isotope separation using graphene-oxide membranes. Carbon, 2022, 186, 344-354.	5.4	15
69	Vortex fluidic induced mass transfer across immiscible phases. Chemical Science, 2022, 13, 3375-3385.	3.7	15
70	Hydrogen induced p-phosphonic acid calix[8]arene controlled growth of Ru, Pt and Pd nanoparticles. Chemical Communications, 2014, 50, 15167-15170.	2.2	13
71	Microwave-assisted shock synthesis of diverse ultrathin graphene-derived materials. Materials Chemistry Frontiers, 2019, 3, 1433-1439.	3.2	13
72	Preparation and Applications of Fluorinated Graphenes. Journal of Carbon Research, 2021, 7, 20.	1.4	13

#	Article	IF	CITATIONS
73	Structural insights into hydrogenated graphite prepared from fluorinated graphite through Birchâ``type reduction. Carbon, 2017, 121, 309-321.	5.4	12
74	Unravelling the structure of the C ₆₀ and p-Bu ^t -calix[8]arene complex. Chemical Communications, 2015, 51, 11413-11416.	2.2	11
75	Stage-1 cationic C60 intercalated graphene oxide films. Carbon, 2021, 175, 131-140.	5.4	11
76	Room temperature vortex fluidic synthesis of monodispersed amorphous proto-vaterite. Chemical Communications, 2014, 50, 11764-11767.	2.2	10
77	Synthesis of few-layer graphene by lamp ablation. Carbon, 2015, 94, 349-351.	5.4	10
78	Plasma enhanced vortex fluidic device manipulation of graphene oxide. Chemical Communications, 2016, 52, 10755-10758.	2.2	10
79	Modification of the Interlayer Coupling and Chemical Reactivity of Multilayer Graphene through Wrinkle Engineering. Chemistry of Materials, 2021, 33, 2506-2515.	3.2	10
80	Ruthenium Complexes in Homogeneous and Heterogeneous Catalysis for Electroreduction of CO ₂ . ChemCatChem, 2020, 12, 1292-1296.	1.8	9
81	F-diamane-like nanosheets from expanded fluorinated graphite. Applied Surface Science, 2022, 583, 152534.	3.1	8
82	Calixarene-mediated assembly of water-soluble C ₆₀ -attached ultrathin graphite hybrids for efficient activation of reactive oxygen species to treat neuroblastoma cells. Chemical Communications, 2020, 56, 7325-7328.	2.2	7
83	One-Step Photochemical Synthesis of Transition Metal–Graphene Hybrid for Electrocatalysis. ACS Sustainable Chemistry and Engineering, 2019, 7, 4112-4118.	3.2	6
84	Flash-assisted doping graphene for ultrafast potassium transport. Nano Research, 2022, 15, 4083-4090.	5.8	6
85	p-Phosphonic acid calix[8]arene mediated synthesis of ultra-large, ultra-thin, single-crystal gold nanoplatelets. Chemical Communications, 2019, 55, 3785-3788.	2.2	5
86	Nitrate uptake by p-phosphonic acid or p-(trimethylammonium)methyl calix[8]arene stablized laminar materials. RSC Advances, 2014, 4, 48348-48352.	1.7	3
87	Metal–Sulfur Linkages Achieved by Organic Tethering of Ruthenium Nanocrystals for Enhanced Electrochemical Nitrogen Reduction. Angewandte Chemie, 2020, 132, 21649-21653.	1.6	3
88	Spatially confined atomic dispersion of metals in thermally reduced graphene oxide films. Carbon, 2022, 188, 367-375.	5.4	2
89	Graphite-Mediated Microwave-Exfoliated Graphene Fluoride as Supercapacitor Electrodes. Nanomaterials, 2022, 12, 1796.	1.9	2
90	Liquid interface evolution of polyhedral-like graphene. Chemical Communications, 2015, 51, 14609-14612.	2.2	1